

1
2
3
4
5
6
7
8
9
10
11
12
13
14
15
16
17
18
19
20
21
22
23
24
25
26
27
28
29

DR. PATRICK MAHONEY (Orcid ID : 0000-0002-2715-3096)

Article type : Original Paper

The Biorhythm of Human Skeletal Growth

Patrick Mahoney¹, Justyna J. Miskiewicz², Simon Chapple¹, Mona Le Luyer^{1,3}, Stephen H. Schlecht⁴, Tahlia J. Stewart², Richard A. Griffiths⁵, Chris Deter¹, Debbie Guatelli-Steinberg⁶

¹Human Osteology Lab, Skeletal Biology Research Centre, School of Anthropology and Conservation, University of Kent, Canterbury, UK.

²Skeletal Biology and Forensic Anthropology Research Group, School of Archaeology and Anthropology, Australian National University, Canberra, Australia.

³De la Préhistoire à l'Actuel Culture Environment et Anthropologie (PACEA), University of Bordeaux, Aquitaine, France.

⁴Department of Orthopaedic Surgery, University of Michigan, Ann Arbor, MI, USA.

⁵Durrell Institute of Conservation and Ecology, School of Anthropology and Conservation, University of Kent.

⁶Department of Anthropology, The Ohio State University, Columbus, OH, USA .

Correspondence

Patrick Mahoney. Human Osteology Lab, Skeletal Biology Research Centre,
School of Anthropology and Conservation,
University of Kent, Canterbury. UK. CT2 7NR.

E: p.mahoney@kent.ac.uk

T: +44 1227 764 7927

This is the author manuscript accepted for publication and has undergone full peer review but has not been through the copyediting, typesetting, pagination and proofreading process, which may lead to differences between this version and the [Version of Record](#). Please cite this article as [doi: 10.1111/joa.12709](https://doi.org/10.1111/joa.12709)

This article is protected by copyright. All rights reserved

30 Text pages = 19 + bibliography = 6

31 Figures = 6

32 Tables = 2

33 Supporting information = 1

34

35 **Abbreviated title**

36 The biorhythm of human skeletal growth

37

38 **KEYWORDS**

39 Retzius line periodicity. Enamel thickness. Daily enamel secretion rates. Osteocyte lacunar density.

40 Stature.

41

42

43 **Abstract**

44 Evidence of a periodic biorhythm is retained in tooth enamel in the form of Retzius lines.
45 The periodicity of Retzius lines (RP) correlates with body mass and the scheduling of life
46 history events when compared between some mammalian species. The correlation has led to
47 the development of the inter-specific Havers-Halberg Oscillation (HHO) hypothesis, which
48 holds great potential for studying aspects of a fossil species biology from teeth. Yet, our
49 understanding of if, or how the HHO relates to human skeletal growth is limited. The goal
50 here is to explore associations between the biorhythm and two hard tissues that form at
51 different times during human ontogeny, within the context of the HHO. First, we investigate
52 the relationship of RP to permanent molar enamel thickness and the underlying daily rate that
53 ameloblasts secrete enamel during childhood. Following this, we develop preliminary
54 research conducted on small samples of adult human bone by testing associations between
55 RP, adult femoral length (as a proxy for attained adult stature), and cortical osteocyte lacunae
56 density (as a proxy for the rate of osteocyte proliferation). Results reveal RP is positively
57 correlated with enamel thickness, negatively correlated with femoral length, but weakly
58 associated with the rate of enamel secretion and osteocyte proliferation. These new data
59 imply that a slower biorhythm predicts thicker enamel for children but shorter stature for
60 adults. Our results develop the intra-specific HHO hypothesis suggesting that there is a
61 common underlying systemic biorhythm that has a role in the final products of human enamel
62 and bone growth.

63
64
65
66
67
68
69
70
71
72
73
74
75
76
77
78
79
80
81
82
83
84
85
86
87
88
89
90
91
92
93
94
95
96

Introduction

Biorhythms are cyclic changes in an organism's growth, development, or functioning that are driven by an internal biological 'clock' and synchronized through environmental cues (Hastings, 1998). They have been linked to variations in human body temperature, metabolism, testosterone production, ovulation, and rate of tooth eruption (Reinberg et al., 1965; Little and Rimmel, 1971; Sothorn, 1974; Lee and Profitt, 1995; Garde et al., 2000). Human tooth enamel retains evidence of periodic fluctuations that occur as enamel forming cells (secretory ameloblasts) deposit mineralising protein matrix (Retzius, 1837; Asper, 1916). One of these fluctuations manifests as cross striations, which are incremental enamel markings that correspond with a circadian rhythm (Schour and Poncher, 1937; Boyde, 1979, 1989; Risnes, 1986; Bromage 1991; Antoine et al., 2009; Lacruz et al., 2012; Zheng et al., 2013). Another longer-period infradian rhythm leads to enamel Retzius lines (e.g., Dean, 1987; Risnes, 1990; Beynon, 1992). Retzius lines mark 'layers' of forming enamel that are usually separated by six to 12 days of growth in human permanent teeth (**Fig. 1**), depending upon the individual (Schwartz et al., 2001; Reid and Dean, 2006; Reid and Ferrell, 2006; Mahoney, 2008). The Havers Halberg Oscillation (HHO) hypothesis proposes that Retzius line periodicity (RP), the number of days between adjacent Retzius lines, is a manifestation of a central infradian biorhythm that regulates the rate of bone cell proliferation and adult body mass via metabolism, with links to life history traits, when compared between some mammalian species (Bromage et al., 2009, 2012). Much less is known about the potential role of this oscillation for human skeletal growth. Here, we extend our previous intra-specific research into the HHO in which we established associations between human deciduous enamel growth and RP (Mahoney et al., 2016; 2017). We construct and test predictions about the relationship of RP to human permanent enamel thickness and the underlying daily rate that enamel forms during the childhood years. We develop preliminary research conducted on small samples of adult human bone (Bromage et al., 2016a), by assessing the relationship of

97 adult femoral length and the underlying density of bone maintenance cells (osteocytes) to RP.
98 Our goal is to explore the periodicity of the biorhythm against two hard tissues that form at
99 different but overlapping times during human ontogeny, within the context of the HHO.

100

101 **Enamel biorhythms of mammals and the Havers-Halberg Oscillation hypothesis**

102 Research into relationships between the periodicity of Retzius lines and somatic growth
103 commenced in the 1990's with those that suspected RP might relate to mammalian body size
104 (Dean, 1995; Dean and Scandrett 1996). Soon after, studies established a significant inter-
105 specific positive correlation between RP and average body mass in a selection of extant and
106 fossil mammals (Smith et al., 2003; Smith, 2008; Bromage et al., 2009). Not all primate
107 species followed this pattern (Hogg et al., 2015), and a lower rather than a higher RP related
108 to a larger estimated body mass for three fossil species (Schwartz et al., 2002, 2005; Le
109 Cabec et al., 2017). Further work reported inter-specific associations between the periodicity
110 of the biorhythm and the scheduling of life history traits for some primate species (Bromage
111 et al., 2012). The inter-specific HHO hypothesis developed out of these studies, and earlier
112 research on mammals (Mullender et al., 1996; Bromage et al., 2009, 2012).

113 The biological 'clock' that regulates Retzius lines is unknown. Given that RP subdivides
114 into multiples of daily intervals, the suprachiasmatic nucleus of the hypothalamus (SCN) has
115 been identified as one likely contender (Bromage et al., 2012). The SCN is a source of
116 circadian rhythmic activity in mammals (Richter, 1965; Ralph et al., 1990; Sujino et al.,
117 2003), has been linked to the circadian production of dentin (Ohtsuka-Isoya, 2001), and also
118 has a role in regulating metabolism via the pituitary gland (Weaver, 1998; Kalsbeek et al.,
119 2011; Coomans et al., 2013). The HHO hypothesis drew upon this biological pathway
120 proposing that Retzius lines were a manifestation of a longer-period oscillation stemming
121 from the hypothalamus that employed SCN 'machinery' in its pathway to stimulate pituitary
122 secretions that linked to metabolism, body mass, and primate life history traits (Bromage et
123 al., 2012). Experimental research on domestic pig links aspects of metabolism to RP
124 (Bromage et al., 2016b). Further support for an inter-specific HHO is provided by some
125 mammalian species with slower metabolisms, and a larger body size combined with a higher
126 mean RP, relative to those with smaller body size (Bromage et al. 2009).

127

128 **Enamel biorhythms of humans and the Havers-Halberg Oscillation hypothesis**

129 The idea that human enamel growth might be controlled by an underlying biological 'clock'
130 is not a new one, as the presence of daily cross-striations along enamel prisms implies that
131 secretory ameloblasts may be under circadian control via clock genes (maintainers of

132 circadian rhythms) during amelogenesis (Schour and Poncher, 1937; Bromage, 1991; Antoine
133 et al., 2009; Lacruz et al., 2012; Zheng et al., 2013). However, much less is known about the
134 potential role of the longer-period HHO for human enamel growth. Recently we reported
135 links between RP, the width of enamel 'layers' between adjacent Retzius lines, and two
136 dimensional (2D) average and relative enamel thickness of human deciduous maxillary
137 second molar crowns (dm^2) (Mahoney et al., 2016, 2017). We also identified an association
138 between RP and dm^2 paracone cusp formation time (Mahoney et al., 2016). The relationship
139 of RP to daily enamel secretion rates (DSRs) was however less clear. When RP and DSRs
140 were calculated for dm^2 in one homologous dental location and compared between
141 individuals there was a weaker association between these variables (Mahoney et al., 2017).
142 Prior to our research, enamel growth had not been considered within the context of the HHO
143 hypothesis. Based upon our data, we proposed that if RP is evidence of the HHO, an
144 underlying biorhythm that affects physiological systems (Bromage et al., 2009, 2012), then
145 its influence extends to enamel thickness and formation time of deciduous molar enamel, but
146 was less clearly associated with deciduous DSRs (Mahoney et al., 2017). Up until now, no
147 study has determined if there is a relationship between RP and human permanent molar
148 enamel thickness, or DSRs calculated for this tooth type.

149 Research on four adult humans hints at a negative correlation between adult stature and
150 RP (Bromage et al., 2016a). This shift away from the positive correlation reported in inter-
151 specific research on mammalian species (see above) is to be expected within the context of
152 the HHO. Inter-specifically, mammals with larger bodies tend to have an extended growth
153 period with slower rates of metabolism and associated cell proliferation, which is reflected by
154 a higher mean RP (and thus slower oscillation of the biorhythm) relative to smaller bodied
155 species (Mullender et al., 1996; Bromage et al., 2009). Within humans, the growth period is
156 constrained between birth and adulthood, so greater stature is achieved by 'speeding up' the
157 biorhythm (reducing the periodicity), and thus increasing skeletal metabolism or the rate of
158 cell proliferation (Bromage et al., 2016a). Thus, our current understanding of the HHO is
159 that inter-specific scaling trends between RP and body size may be associated with alterations
160 in the *duration* of development, whereas within humans, RP may relate to adult stature
161 through variation in growth *rates* (Bromage et al., 2009).

162 Preliminary support for the HHO hypothesis within humans is provided by a study of
163 bone osteocyte lacunar density (Ot.Dn) (Bromage et al., 2016a). Osteocytes are former
164 osteoblasts that become trapped as they finish producing bone matrix (e.g., Palumbo et al.,
165 1990). These cells have a complex functionality, that includes sensing mechanical (shear or

166 strain) forces applied to bone, which activates remodeling via the linked action of osteoblasts
167 and osteoclasts (e.g, Frost, 1987; Robling and Turner, 2002; Mullender et al., 2007;
168 Bonewald, 2007; Tatsumi et al., 2007; Noble, 2008); detecting and initiating micro-damage
169 repair (e.g., Verborgt et al., 2000; Herman et al., 2010); and in mineral homeostasis (e.g.,
170 Cullinane, 2002; Teti and Zallone, 2009; Nakashima et al., 2011). The Ot.Dn of healthy bone
171 can also vary when compared to pathological bone (e.g., Mullender et al; 2005; van Hove et
172 al, 2009). In addition to these potential influences, Ot.Dn can correspond with body size,
173 whereby Ot.Dn of the mid-shaft femur from 12 adult humans scaled positively with final
174 attained adult stature (Bromage et al., 2016a). This scaling relationship suggests that the rate
175 of osteocyte proliferation is greater in taller adult individuals, which is consistent with the
176 hypothesised effect of the HHO on human body size.

177

178 **Research questions and predictions**

179 The background research provides a foundation from which to formulate four research
180 questions, and from these, predictions, that will be tested by calculating RP from thin sections
181 of teeth and comparing these values to measures of human skeletal growth. The research
182 questions are as follows:

183

184 ***Do daily enamel secretion rates correlate with RP in permanent molars?***

185 We have previously shown RP does not exert a consistent influence on the daily rate that
186 ameloblasts secrete structural matrix proteins as they increase the length of hydroxyapatite
187 crystallites in deciduous enamel (Mahoney et al., 2017). Instead, it seems more likely from
188 links we have reported, and by others, that the intra-specific HHO is related to the end state
189 of enamel growth (i.e., final enamel thickness) through formation time. These links
190 commence as ameloblasts secrete matrix for an additional number of days between adjacent
191 Retzius lines, leading to thicker 'enamel layers' with higher RP's (Mahoney et al., 2017).
192 Layers become thicker because ameloblasts do not greatly alter their DSRs as RP increases,
193 when compared between outer lateral enamel regions of human molars from different
194 individuals. Thicker layers accumulate leading to greater average enamel thickness (AET) of
195 dm² crowns with higher RP's, relative to molars with lower RP's (Mahoney et al. 2016).
196 Thicker crown enamel takes a longer period of time to form, for deciduous molars (Mahoney
197 2011), and permanent teeth (Dean et al., 2001). Formation time is correlated with RP, for
198 deciduous molar paracone cusps (Mahoney et al., 2016) and for permanent mandibular canine
199 lateral enamel (Reid and Ferrell, 2006). Thus, unlike the HHO intra-specific prediction for
200 body mass, where RP links to final attained adult stature through variation in growth rates

201 (Bromage et al., 2009), we suggest that RP is not strongly related to final enamel thickness
202 via daily enamel secretion rates (and is thus more likely to be related to enamel formation
203 time). Thus, we predict a weak association between RP and DSRs of permanent molars. To
204 examine the relationship between the circadian and the infradian rhythm in permanent
205 enamel, we separated out $n=15$ M1's from our sample, and calculated and compared RPs and
206 DSRs in one homologous location in outer lateral enamel of each crown.

207

208 ***Does permanent molar enamel thickness correlate with RP?***

209 Two dimensional measurements of AET from human dm^2 correlated positively with RP
210 (Mahoney et al., 2016). Assuming that RP is evidence of a biorhythm that affects multiple
211 physiological systems, including enamel growth, then we predict that its influence will extend
212 to permanent molar enamel thickness. To test this prediction we calculate 2D AET and
213 enamel area (EA) for human permanent first (M1) and second molars (M2) from thin
214 sections, and compare these values to RP's of the same teeth. Based upon findings for
215 deciduous molars, RP of permanent molars should scale positively with our measures of
216 enamel thickness.

217

218 ***Is adult femoral length correlated with RP?***

219 The intra-specific HHO predicts that greater adult height is achieved through a biorhythm
220 that is accelerated (Bromage et al. 2016a), with a shorter periodicity. To assess RP against
221 stature, we selected a sample of younger adult males with shorter femora, and compared these
222 to younger adult males with longer femora. We calculated RP for each male and compared
223 this value to his stature (reconstructed from femoral length). The femur has been used within
224 regression equations for the past fifty years to reconstruct stature (e.g., Trotter, 1970; and see
225 methods). We also compare RP to femoral length.

226

227

228

229

230

231

232 ***Is adult femoral length correlated with cortical bone osteocyte lacunae density?***

233 The intra-specific HHO predicts that taller humans (with longer femora) grow more rapidly
234 with a faster rate of osteocyte proliferation, relative to shorter individuals. Data for 12
235 individuals indicate these faster rates are then maintained as adults (Bromage et al., 2016a).
236 As Ot.Dn can sometimes vary with age (e.g., Mullender et al., 1996) we subdivided our entire
237 adult male sample into age groups and explored associations between Ot.Dn and stature,
238 within each group. We also assess Ot.Dn against adult femoral length, and against RP.

239

240 **Materials and Methods**

241 Our samples are human skeletons from one cemetery in Canterbury, England, that dates to
242 the early 16th century AD (Hicks and Hicks, 2001). Historical texts state that burials were
243 from a single lower socio-economic group that lived and worked in Canterbury and
244 represented non-catastrophic mortality (Somner 1703; Duncombe 1785; Brent 1879). We
245 have previously shown that the periodicity of the biorhythm can change in response to non-
246 specific pathology (Mahoney, et al., 2017). We limited this type of variation in our data by
247 only selecting skeletons and teeth without skeletal or radiographic signs of pathology,
248 drawing upon an extensive collection of accompanying radiographs that were produced at
249 Kent and Canterbury Hospital (Radiology Department) for any skeleton with suspected
250 trauma or pathology. Age-at-death is reconstructed for all skeletons; sex is reconstructed for
251 adults (see Methods). These collections are curated in the Skeletal Biology Research Centre,
252 University of Kent, UK. All sectioning adhered to the British Association of Biological
253 Anthropology and Osteoarchaeology code of practice (2014). No permits were required for
254 this study as these are archaeological samples from before the 19th Century AD.

255
256
257
258
259

260 **Samples and the chronology of skeletal growth**

261 We selected three samples. Throughout, RP is calculated for lateral enamel of permanent M1
262 and M2. Lateral enamel of these tooth types forms between approximately 1.5 to 5.7 years of
263 age (Reid and Dean, 2006). Sample sizes varied depending upon the variables examined and
264 are given in the corresponding tables. One tooth (either M1 or M2) represents one individual.
265 Raw data is available in Supporting Information.

266

267 **a)** The first sample was juveniles ($n=40$). We assessed RP against daily enamel secretion
268 rates, and against enamel thickness of the same molars. We chose juveniles (<8yrs of age
269 for M1's; <13yrs for M2's) because enamel is often worn in adults, and this would have
270 affected our measurements of 2D AET and EA. Daily enamel secretion rates of M1 and
271 M2 are a measure of the rate at which ameloblasts previously deposited matrix during the
272 secretory phase of enamel growth in the childhood years. Average enamel thickness and
273 EA of M1 and M2 are a measure of the end state of the secretory stage of enamel growth
274 that is attained in childhood.

275

- 276 **b)** The second sample was young adult males, aged between 18 to 34yrs ($n=27$). We
277 assessed RP of their M1 or M2 (representing their childhood years), against their femoral
278 cortical bone osteocyte lacunar density, and final attained adult stature. Osteocyte
279 lacunar density in adult cortical bone likely represents a combination of lamellae
280 deposited during later ontogeny and in adulthood. Final attained adult stature is the end
281 state of linear growth of long bones via endochondral ossification over the course of
282 postnatal development from birth to adulthood. In this study, we measure adult femoral
283 length as a proxy for attained adult stature. The slight occlusal wear of some molars did
284 not affect our calculation of RP in lateral enamel, which is located cervical to wear on
285 the occlusal surface. We did not include older adults because of their greater enamel
286 wear.
- 287 **c)** The third sample was adult males, subdivided into two age groups (younger males 18-
288 34yrs, $n=28$; older males 35-50yrs, $n=94$). We assessed femoral cortical Ot.Dn against
289 their estimated stature, and femoral length.

290

291 **Sample preparation for histology**

292 We used standard histological techniques (Bancroft and Gamble, 2008; Mahoney, 2008;
293 Miskiewicz, 2016). Each tooth was embedded in polyester resin to reduce the risk of
294 splintering while sectioning. Using a diamond-wafering blade (Buehler® IsoMet 4000
295 precision saw), buccal-lingual sections captured the paracone and protocone of maxillary
296 molars and the protoconid and metaconid of mandibular permanent molars. Each section was
297 mounted on a microscope slide, lapped using a graded series of grinding pads (Buehler®
298 Eco-Met 300) to reveal incremental lines, polished with a $0.3\mu\text{m}$ aluminum oxide powder
299 (Buehler® Micro-Polish II), placed in an ultrasonic bath to remove surface debris, dehydrated
300 through a series of alcohol baths, cleared (Histoclear®), and mounted with a coverslip using a
301 xylene-based mounting medium (DPX®).

302 Dry, un-decalcified bone measuring 1cm in depth was removed from the posterior
303 femoral mid-shaft cortex using a drill (Dremel Rotary®) with a circular metal blade (**Fig. 2**).
304 Only the posterior portion of the femoral diaphysis was used in order to keep the overall
305 integrity of the femur preserved for future research purposes. The bone was embedded in
306 epoxy resin, reduced in thickness (Buehler® IsoMet 4000 precision saw), ground, polished,
307 and cover-slipped following the same procedures used to embed and prepare the teeth. Thin
308 sections measured approximately $100\mu\text{m}$ in depth.

309

310

311

312
313
314
315

316 **Retzius line periodicity**

317 Using a high-resolution microscope (Olympus® BX51), each section was examined at
318 magnification (10-60x). Images were captured with a microscope digital camera (Olympus®
319 DP25) and analyzed in CELL® Live Biology imaging software. We counted the number of
320 cross-striations along a prism between several adjacent Retzius lines in outer lateral enamel
321 of M1 and M2 to determine the number of days between two adjacent Retzius lines. For
322 twelve thin sections, cross-striations were not clearly visible and continuous along prisms
323 between adjacent Retzius lines. For these twelve sections, we divided the distance between
324 several adjacent Retzius lines by local mean daily secretion rates (e.g., Schwartz et al., 2001;
325 Mahoney et al., 2007; Lacruz et al., 2008). We did not include these sections in the analysis
326 of RP and secretion rates. Retzius periodicity was recorded by SC and PM. Intraclass
327 correlation coefficient of 0.996 (n= 40; 95% CI= 0.993-0.998; $p=0.000$) indicates a high
328 degree of agreement between the two observers, with one difference in RP calculations. This
329 slide was removed from the study.

330

331 **Enamel thickness**

332 The 2D AET in mm was calculated by dividing the area of the enamel cap (EA) by the length
333 of the dentin-enamel junction (DEJ), which provides the average straight-line distance
334 between the DEJ and outer enamel surface (Martin, 1983, 1985). EA is given in mm^2 .

335

336 **Enamel daily secretion rates**

337 Secretion rates in μm per day were calculated for outer lateral enamel in the same region that
338 we recorded RP (ie., avoiding inner and mid enamel regions as DSRs can vary from one
339 region to the next within a crown: Lacruz and Bromage 2006). Rates were measured along
340 the long axis of an enamel prism. A distance corresponding to five days of enamel secretion
341 was measured, and then divided by five to yield a mean daily rate. The procedure was
342 repeated a minimum of six times in each region, which allowed a grand mean value and
343 standard deviation (SD) to be calculated. The grand mean value was compared to RP
344 calculated in the same enamel region.

345

346 **Osteocyte lacunae density**

347 We use Ot.Dn as a proxy for the rate of (past) femoral cortical bone cell proliferation.
348 Osteocyte lacunae density data were collected as part of a PhD project (Miszkievicz, 2014).
349 We selected femoral Ot.Dn, rather than osteon population density, so that we could directly

350 test prior research (see above). Osteocyte lacunae density is significantly correlated with
351 osteon population density in this skeletal sample (Miszekiewicz, 2016). Exploring associations
352 between Ot.Dn and age, or at the initiation of remodeling (e.g., Metz et al., 2003), were not
353 aims of this study.

354 Using a high-resolution microscope (Olympus® BX51, and Olympus DP25 microscope
355 camera) osteocyte lacunae were counted within secondary osteonal bone and interstitial bone.
356 Ot.Dn were counted from a maximum of six main regions of interest (ROI; mag =10X, 2.44
357 mm²) positioned adjacent to the periosteum, and sub-divided into smaller ROIs (mag =40X,
358 0.13 mm²) (Fig. 2). See Miszekiewicz (2016) for a detailed methodology of ROI's. Using
359 CELL® Live Biology Imaging software, all visible osteocyte lacunae (including cavities
360 which appeared “empty” or transparent) were counted using a “touch count” tool (identical in
361 premise to the “point count technique” recommended by Parfitt, 1983). Densities were
362 calculated by dividing the total number of osteocyte lacunae by the area of bone examined (in
363 mm²). We acknowledge that automated methods of osteocyte lacunae detection are available,
364 and ideally a whole long bone cross-section should be examined (e.g. Hunter and Agnew,
365 2016). However, those techniques are better suited to fresh or “recent” bone with excellent
366 microstructural preservation. Given the archaeological background (localised diagenetic
367 alteration of micro-anatomy) of our samples, there needed to be flexibility in our ROI
368 selection procedures. This is because the ROI would sometimes have to be moved
369 fractionally to avoid an area of diagenesis or one that was affected by taphonomy. Clear
370 differences in osteocyte lacunar densities were observed across the sample (see Fig. 2).

371

372 **Stature estimation and femoral length**

373 Femoral length data were previously included in robusticity index calculations as part of
374 another project (Miszekiewicz and Mahoney, 2016), but correlations between Ot.Dn and
375 stature/femur length are examined here for the first time. The maximum length of each femur
376 was measured by placing it flat on an osteometric board, in its anatomical position, with the
377 posterior femoral aspect facing down. Femoral length was measured from the most superior
378 surface of the femoral head to the most distal surface of the medial condyle (Buikstra and
379 Ubelaker, 1994). Standard, and most commonly used formulae for reconstructing stature in
380 skeletal remains were used (Trotter, 1970; White et al., 2011). These were specific to sex and
381 appropriate for individuals of European descent. Male stature was estimated using the
382 regression equation: $2.38 \times \text{femur maximum length in cm} + 61.41 (+/- 3.27)$ (Trotter, 1970;
383 White et al., 2011).

384

385 **Sex determination and age-at-death**

386 Sex determination was carried out using multiple standard methods to increase the accuracy
387 of the determination. We relied upon standard morphological characteristics of the pelvis and
388 cranium. The pelvic methods were based upon 25 morphological characteristics of the human
389 pelvis taken from Schwartz (1995), Ferembach et al., (1980), Krogman and Iscan (1986) and
390 Phenice (1969). Cranial features included the mastoid process, supraorbital margin, mental
391 eminence, and nuchal crest (Buikstra and Ubelaker, 1994). When determinations from cranial
392 and pelvic features conflicted, priority was given to the pelvic criteria (White et al., 2011). In
393 the analyses, 'probable males' were classified as male.

394 Age was estimated from age-specific morphology of the pubic symphysis, and the
395 auricular surface of the pelvis (e.g., Meindl et al., 1985; Lovejoy et al., 1985). Two age
396 categories were constructed: younger adult males, 18-34 years; older adult males 35-50 years.

397
398

399 **Analyses**

400 Data were analyzed in IBM SPSS® 22 (2014). Each variable was log-transformed. A one
401 sample Kolmogorov-Smirnov test indicated that the distribution of the data for each variable
402 was normal. Data from right and left femora (one femur was selected from each individual,
403 and either the right or left depending upon preservation) were pooled. We analyze the data
404 using linear regression statistics. In Tables 1-2 we present the r^2 value (coefficient of
405 determination) which measures the proportion of explained variation, and we also show the r
406 value (correlation coefficient) which measures the strength and direction of the relationship
407 between variables. The residual, presented as a percentage in the Tables, is the error not
408 explained by the regression equation.

409

410

411

412

413

414

415

416

417

418

419

420

421 **Results**

422 **Retzius line periodicity, enamel thickness and secretion rates**

423 Regression statistics are in Table 1. Corresponding data for the sample of juveniles is
424 available in Supporting Information Table S1. When data for all tooth types are combined,
425 the enamel areas and AET of permanent molar crowns were significantly and positively
426 related with RP, increasing from minimum values that were associated with an RP of 6 days
427 to maximum values that were associated with RP's of 10 and 11 days respectively (**Fig 3a.**
428 **Fig 4a**). When subdivided into either M1's or M2's and re-analyzed, RP was significantly
429 related to EA and AET (Table 1). When further subdivided into upper or lower molars, RP
430 was significantly related to EA (**Fig 4b-d**). AET was also significantly related to RP for each
431 upper and lower molar type, except lower M2 where this relationship approached
432 significance ($r^2=0.287$; $p=0.072$).

433 When 15 permanent first molars were separated from the sample, and RPs and DSRs
434 were measured and compared between the molars in one homologous location in outer lateral
435 enamel of each crown, there was no consistent or significant association with the periodicity
436 of Retzius lines.

437

438 **Retzius line periodicity, femoral length and osteocyte lacunae density**

439 Regression statistics are in Table 2. The corresponding data sets for younger and older male
440 adults are available in Supporting Information Table S2 and Table S3. Estimated stature (and
441 femoral length) was significantly and negatively related with RP (**Fig. 3b**). The density of
442 osteocyte lacunae did not relate significantly with RP (Table 2). Osteocyte lacunae density
443 was not significantly related to femoral length, or stature for younger males (Table 2). There
444 was a weak relationship between Ot.Dn and stature that approached significance in older
445 males though the residual was high ($r^2=0.030$; $p=0.089$).

446

447 **Discussion**

448 This study builds upon our previous work that examined relationships of RP to human
449 deciduous molar enamel growth, and extends preliminary research into associations between
450 RP and human adult femoral cortical bone growth (Bromage et al., 2016a; Mahoney et al.,
451 2016, 2017). We examined the relationship of permanent molar daily enamel secretion rates
452 to RP, and of osteocyte proliferation to RP. We find limited evidence for either of these

453 relationships, but did find stronger evidence of linkages between RP, permanent molar
454 enamel thickness, and stature.

455

456 **Retzius line periodicity, enamel thickness and secretion rates**

457 Our data support the prediction that the periodicity of the biorhythm is associated with
458 enamel thickness when considered within a smaller intra-specific scale, within humans.
459 However, as with deciduous molars (Mahoney, et al., 2016), RP was more weakly associated
460 with DSRs, when compared between permanent molars from different individuals. Therefore,
461 even though RP is calculated by a count of cross striations, variation in the biorhythm is not
462 always associated with the *amount* of matrix deposited by ameloblasts in 24 hour periods
463 (**Fig. 5**). Instead, it seems likely that RP can link to the final enamel thickness of a human
464 crown through formation time. RP is related to the time taken to form part of a deciduous
465 and permanent tooth crown (Reid and Ferrell, 2005 Mahoney et al., 2016), and formation
466 time is related to human enamel thickness (Dean et al., 2001; Mahoney 2011). Thus, inter-
467 individual variation in the periodicity of the biorhythm may have a clearer association with
468 final enamel thickness through the duration, rather than the daily rate of enamel growth. More
469 work is needed to understand if and how these developmental mechanisms change within a
470 species (**Fig 5**).

471 The proposal that aspects of enamel growth are controlled by a long-period biological
472 ‘clock’ with an infradian rhythm, whether it is the HHO via the SCN of the brain, or a
473 different ‘peripheral’ independent ‘clock’ (Hastings, 1998), or even more than one ‘clock’
474 (Newman and Poole, 1974, 1993), is a hypothesis. Our data for human permanent teeth, and
475 deciduous teeth (Mahoney et al., 2016, 2017), provide support for this hypothesis. The
476 infradian rhythm (reflected by RP) appears to have an association with final enamel thickness
477 of a crown, but is inconsistently related to the daily *amount* of enamel secreted by
478 ameloblasts as these cells respond to a circadian rhythm (reflected by cross striations). The
479 infradian rhythm likely has a systemic origin, as RP can alter within a single crown in
480 response to non-specific pathology (Mahoney et al., 2017). The longer-period rhythm is
481 intrinsic to enamel growth, not only relating to final enamel thickness, but also the
482 microstructural components of enamel (prisms) which can be reduced in size, or have an
483 altered morphology when associated with Retzius lines (Risnes, 1990,1998; Li and Risnes,
484 2004). Perhaps therefore, the infradian rhythm periodically modifies ameloblast metabolism,
485 interfering with enamel secretion of ameloblasts, leading to the altered prism structure that
486 can be associated with Retzius lines.

487 There is substantial residual in the relationship of RP to enamel thickness (Table 1), as
488 even the strongest correlations explain just over half of the variation in our data. So, there are
489 other factors operating as well. Enamel thickness is a product of several mechanisms, other
490 than those considered here, such as the number of active ameloblasts and their life spans
491 (Grine and Martin, 1988; Macho, 1995). We have only considered the rate that enamel grows
492 in thickness, but whether the rate that enamel crowns extend in height (enamel extension
493 rates), as epithelium cells differentiate into pre-ameloblasts down along the dentin-enamel
494 junction (DEJ), is linked to RP, has yet to be determined. Guatelli-Steinberg and colleagues
495 (2012) have already shown links between DEJ lengths and lateral enamel formation time. As
496 RP is correlated with enamel formation times (Reid and Ferrell, 2006; Mahoney et al., 2016),
497 it would seem possible that extension rates can relate to RP.

498

499 **Retzius line periodicity, femoral length, and osteocyte lacunae density**

500 Our data support the intra-specific HHO prediction that taller adults (with longer femora)
501 have a lower RP (Bromage et al., 2016a). Thus, the biorhythm oscillates with a faster
502 periodicity in taller humans, compared to those with shorter femora. However, we found less
503 support for the prediction that taller adults maintain significantly faster rates of femoral
504 osteocyte proliferation, relative to shorter adults. Osteocyte density did not relate to stature
505 or femoral length amongst our sample of young adult males, though it appeared to be
506 trending towards significance with a high residual amongst older males (Table 2, and
507 footnotes). Neither did RP relate to Ot.Dn in a small sample. Thus, the biorhythm is
508 significantly linked to adult stature, but neither the biorhythm nor stature are linked to
509 osteocyte proliferation of the femur.

510 Osteocytes have a complex functionality (see Introduction) that, in addition to potential
511 influences of body size, probably influences their distribution in cortical bone leading to
512 significant variation in their numbers across the femoral shaft (e.g., Carter et al. 2013, 2014).
513 For example, an anatomical region can adapt to mechanical loading, adding and removing
514 new bone tissue in response to loading or disuse (Wolff, 1892; Robling et al., 2001; Burr et
515 al., 2002). Our osteocyte lacunae data are from one anatomical region, the posterior femoral
516 mid-shaft cortex, and just the sub-periosteal pocket, which is where new bone is usually
517 deposited in response to excessive load (Robling et al., 2006). There is substantial inter-
518 individual variation in Ot.Dn values from this region (younger adults range between 394.87
519 and 1307.69; middle aged adults between 305.77 and 1255.13). Some of this variation in
520 Ot.Dn probably reflects differences in femoral mechanical loading between individuals, as

521 some adults in our sample would have been employed in the physically demanding
522 occupations that were typical of lower socio-economic lifestyles in medieval Canterbury
523 (Miszkiewicz and Mahoney, 2016).

524

525 Variation in adult stature is not strongly related to differences among individuals in the
526 rate of femoral osteocyte proliferation, but it is related to RP (Table 2). This finding makes
527 sense if RP is linked to the duration in which stature is attained. Pre-pubertal growth velocity
528 differences can underlie adult stature differences within some populations (e.g., Gasser 1990;
529 Gasser et al., 2001), but not all populations. Instead, the timing of the pubertal growth spurt
530 can contribute to the *age* adult height is attained, for females compared to males (e.g.,
531 Tanner, 1990; Roche, 1992; Gasser et al., 2000), and within the sexes (Hägg and Taranger,
532 1991; Baer et al., 2006). Late maturing Swedish boys continued to grow between 18 to 25
533 years of age, attaining significantly greater growth in height during this period and a greater
534 final stature, compared to early maturing boys whose height increased only slightly after age
535 18 (Hägg and Taranger, 1991). The Nurses' Health Study (II) in the USA, which is based
536 upon large sample sizes, indicates that females with delayed puberty are older when they
537 attain their final and greater adult height, compared to females with a shorter adult stature
538 (Baer et al., 2006). Further research might explore potential linkages between the frequency
539 that the biorhythm oscillates and the age that adult stature is attained, as the duration of the
540 growth period may be an important link to RP for aspects of both enamel and bone growth.
541 Variation in growth velocities (and Ot.Dn) compared to RP amongst children should also be
542 examined.

543

544 **The biorhythm of human skeletal growth**

545 The direction of the correlation between RP and enamel thickness is positive, but negative
546 when RP is related to stature. Our data implies that a child from Canterbury with a slow
547 biorhythm between birth and five or six years of age attained thicker deciduous (Mahoney et
548 al., 2016) and permanent molar enamel, compared to another child with a faster biorhythm
549 that developed thinner enamel (**Fig. 6**). A child from the same population with a fast
550 biorhythm attained a greater adult stature. These findings imply that the biorhythm may
551 coordinate different aspects of human skeletal growth. Perhaps a child with a slow oscillation
552 attains thicker enamel by increasing the duration of crown enamel growth early on in
553 ontogeny, at the expense of subsequent femoral growth in length and attained adult height.

554 Alternatively, the change in the direction of the correlation may reflect a biorhythm that
555 does not remain constant within an individual. We have previously shown that RP can change

556 within an individual at the end of the first post-natal year (Mahoney et al., 2017). The change
557 in RP, from deciduous to permanent molars, suggests that the biorhythm produces a sequence
558 of RPs for an individual, rather than a single and static value. In the present study, we
559 focused on permanent M1s and M2s, whose enamel forms between birth and five to six years
560 of age (Reid and Dean, 2006). It seems likely that RP remains constant during this age-range
561 within an individual, as comparisons between small samples of permanent anterior teeth that
562 form at about the same time as permanent molars (FitzGerald, 1998), as well as comparisons
563 between molar types within four individuals (Reid et al., 1998), reveal no variation in RP.
564 Whether the periodicity of the biorhythm changes in humans beyond 11 years of age, after
565 third molar crown enamel has formed, is unknown. Therefore, the relationship we describe,
566 between RP during the early childhood years and adult stature, might not describe this
567 relationship in later ontogeny, if RP changes closer to adulthood, or, if bone modifies it's
568 response to the biorhythm with age.

569

570 **Conclusion**

571 We examined the relationship of enamel secretion rates to evidence of a biorhythm retained
572 in human teeth as Retzius line periodicity, and of cortical bone osteocyte proliferation to
573 Retzius periodicity. We found only limited evidence for either of these relationships, but we
574 did find stronger evidence of linkages between RP and permanent molar enamel thickness
575 (end state of enamel growth), and RP and final adult stature (end state of linear growth in
576 long bones). Our findings develop the intra-specific HHO hypothesis suggesting that the
577 biorhythm has a role in human skeletal growth and the development of more than one hard
578 tissue.

579 **Conflict of Interest**

580 The authors have no conflict of interest to declare.

581

582 **REFERENCES**

583 **Antoine D, Hillson S, Dean MC** (2009) The developmental clock of dental enamel: a test for the
584 periodicity of prism cross striations and an evaluation of the likely sources of error in histological
585 studies of this kind. *J Anat* **214**, 45–55.

586

587 **von Asper H** (1916) *Über die Braune Retzius sche Parallelstreifung im Schmelz der menschlichen*
588 *Zähne*. PhD thesis: Universität Zurich.

589

590 **Baer HJ, Rich-Edwards JW, Colditz GA, Hunter DJ, Willett WC, Michels KB** (2006) Adult
591 height, age at attained height, and incidence of breast cancer in premenopausal women. *Int J Cancer*
592 **119**, 2231–2235.

593

594 **Bancroft JD, Gamble M** (2008) *Theory and practice of histological techniques*. Elsevier Health
595 Sciences.

596

597 **Beynon AD** (1992) Circaseptan rhythms in enamel development in modern humans and Plio-
598 Pleistocene hominids. In *Structure, Function and Evolution of Teeth* (eds Smith P, Tchernov E), pp.
599 295-309. London: Freund Publishing House Ltd.

600

601 **Boas F** (1935) The tempo of growth of fraternities. *Proc Nat Acad Sci* **21**, 413-418.

602

603 **Bonewald LF** (2007) Osteocytes as dynamic multifunctional cells. *Ann N Y Acad Sci* **1116**, 281–290.

604

605 **Boyde A** (1979) Carbonate concentration, crystal centres, core dissolution, caries, cross striation,
606 circadian rhythms and compositional contrast in the SEM. *J Dent Res* **58**, 981–983.

607

608 **Boyde A** (1989) Enamel. In: *Teeth. Handbook of microscopic anatomy* (eds Berkovitz BKB, Boyde
609 A, Frank RM, et al.), pp. 309–473. Berlin: Springer-Verlag.

610

611 **Brent J** (1879) *Canterbury in the olden time*. London: Simpkin, Marshall and Co.

612

613 **Bromage TG** (1991) Enamel incremental periodicity in the pigtailed macaque: a polychrome
614 fluorescent labelling study of dental hard tissues. *Am J Phys Anthropol* **86**, 205–214.

615

616 **Bromage TG, Hogg RT, Lacruz RS. et al.** (2012) Primate enamel evinces long period biological
617 timing and regulation of life history. *J Theor Biol* **305**, 131–144.

618

619 **Bromage TG, Idaghdour Y, Lacruz RS. et al.** (2016b) The swine plasma metabolome chronicles
620 ‘many days’ biological timing and functions linked to growth. *PLoS One* e0145919.

621

622 **Bromage TG, Juwayeyic YM, Katrisa JA. et al.** (2016a) The scaling of human osteocyte lacuna
623 density with body size and metabolism. *C R Palevol* **15**, 32–39.

624

625 **Bromage TG, Lacruz RS, Hogg R. et al.** (2009) Lamellar bone is an incremental tissue reconciling
626 enamel rhythms, body size, and organismal life history. *Calcif Tiss Int* **84**, 388-404.

627

628 **Buikstra JE, Ubelaker DH** (1994) *Standards for data collection from human skeletal remains.*
629 Fayetteville: Arkansas Archaeology Survey.
630

631 **Burr DB, Robling AG, Turner CH** (2002) Effects of biomechanical stress on bones in animals.
632 *Bone* **30**(5), 781–6.
633 **Le Cabec A, Dean MC, Begun DR** (2017) Dental development and age at death of the holotype of
634 *Anapithecus hernyaki* (RUD 9) using synchrotron virtual histology. *J Hum Evol* **108**, 161-175.
635

636 **Carter Y, Suchorab JL, Thomas CD, Clement JG, Cooper DM** (2014) Normal variation in
637 cortical osteocyte lacunar parameters in healthy young males. *J Anat* **225**, 328-36.
638

639 **Carter Y, Thomas CD, Clement JG, Peele AG, Hannah K, Cooper DM** (2013) Variation in
640 osteocyte lacunar morphology and density in the human femur--a synchrotron radiation_micro-CT
641 study. *Bone* **52**(1), 126-32.
642

643 **Cullinane DM** (2002) The role of osteocytes in bone regulation: mineral homeostasis versus
644 mechanoreception. *J Musc Neuronal Interact* **2**, 242-4.
645

646 **Coomans CP, van den Berg SA, Houben T, van Klinken JB, van den Berg R, Pronk AC,**
647 **Havekes LM, Romijn JA, van Dijk KW, Biermasz NR, Meijer JH** (2013) Detrimental effects of
648 constant light exposure and high-fat diet on circadian energy metabolism and insulin sensitivity.
649 *FASEB J* **27**,1721–1732.

650 **Dean MC** (1987). Growth layers and incremental markings in hard tissues; a review of the literature
651 and some preliminary observations about enamel structure in *Paranthropus boisei*. *J Hum Evol* **16**,
652 157–172.
653

654 **Dean MC** (1995) The nature and periodicity of incremental lines in primate dentine and their
655 relationship to periradicular bands in OH 16 (*Homo habilis*). In *Aspects of Dental Biology:*
656 *Paleontology, Anthropology and Evolution* (ed Moggi-Cecchi J), pp. 239-265. Florence: International
657 Institute for the Study of Man.
658

659 **Dean MC, Leakey MG, Reid DJ. et al.** (2001) Growth processes in teeth distinguish modern
660 humans from *Homo erectus* and earlier hominins. *Nature* **414**, 628–631.
661

662 **Dean MC, Scandrett AE** (1996) The relation between long-period incremental markings in dentine
663 and daily cross-striations in enamel in human teeth. *Arch Oral Biol* **41**, 233-241.
664

- 665 **Duncombe J** (1785) The history and antiquities of the three archiepiscopal hospitals and other
666 charitable foundations at and near Canterbury. *Bibliotheca Topographica Britannica* No XXX,
667 London.
- 668
- 669 **Ferembach D, Schwindezky I, Stoukal M** (1980) Recommendations for age and sex diagnoses of
670 skeletons. *Journal of Human Evolution* 9: 517-549.
- 671
- 672 **FitzGerald CM** (1998) Do enamel microstructures have regular time dependency? Conclusions from
673 the literature and a large scale study. *J Hum Evol* 35, 371-386.
- 674
- 675 **Frost HM** (1987) Bone “mass” and the “mechanostat”: a proposal. *Anat Rec* 219, 1-9.
- 676
- 677 **Gasser T** (1990) A method for determining the dynamics and intensity of average growth. *An Hum*
678 *Biol* 17, 459-457.
- 679
- 680 **Gasser T, Sheehy A, Molinari L, Largo RH** (2000) Sex dimorphism in growth. *An Hum Biol* 27,
681 187-197.
- 682
- 683 **Gasser T, Sheehy A, Molinari L, Largo RH** (2001) Growth processes leading to a large or small
684 adult height. *An Hum Biol* 28, 319-327.
- 685
- 686 **Garde AH, Hansen AM, Skovgaard LT, Christensen JM** (2000). Seasonal and biological variation
687 of blood concentrations of total cholesterol, dehydroepiandrosterone sulfate, hemoglobin A(1c), IgA,
688 prolactin, and free testosterone in healthy women. *Clin Chem* 46(4), 551–559.
- 689
- 690 **Grine FE, Martin LB** (1988) Enamel thickness and development in Australopithecus and
691 Paranthropus. In *The evolutionary history of the robust Australopithecines* (ed Grine FE), pp. 3–
692 42. New York: Aldyne de Gruiter.
- 693
- 694 **Guatelli-Steinberg D, Floyd BA, Dean MC, Reid DJ** (2012) Enamel extension rate patterns in
695 modern human teeth: two approaches designed to establish an integrated comparative context for
696 fossil primates. *J Hum Evol* 63, 475–486.
- 697
- 698 **Hägg U, Taranger J** (1991) Height and height velocity in early, average and late maturers followed
699 to the age of 25: a prospective longitudinal study of Swedish urban children from birth to adulthood.
700 *Ann Hum Bio* 18(1), 47-56.
- 701
- 702 **Hasting M** (1998) The brain, circadian rhythms, and clock genes. *Brit Med J*, 317, 1704-1707.

703

704 **Herman BC, Cardoso L, Majeska RJ, Jepsen KJ, Schaffler MB** (2010) Activation of Bone
705 Remodeling after Fatigue: Differential Response to Linear Microcracks and Diffuse Damage. *Bone*
706 **47**(4), 766–772.

707

708 **Hicks M, Hicks A** (2001) *St. Gregory's Priory, Northgate, Canterbury Excavations 1988–1991*.
709 Canterbury Archaeological Trust Ltd: Volume II.

710

711 **Hogg RT, Godfrey LR, Schwartz GT, Dirks W, Bromage TG** (2015) Lemur biorhythms and life
712 history evolution. *PLoS ONE* **10**(8), e0134210. doi:10.1371/journal.pone.0134210

713

714 **Hunter RL, Agnew AM** (2016) Intrasketal variation in human cortical osteocyte lacunar density:
715 Implications for bone quality assessment. *Bone Reports* **5**, 252-261.

716

717 **Kalsbeek A, Scheer FA, Perreau-Lenz S. et al.** (2011) Circadian disruption and SCN control of
718 energy metabolism. *FEBS Letters* **585**, 1412–1426.

719

720 **Krogman WM, Iscan MY** (1986) *The human skeleton in forensic medicine* (2nd ed). Springfield:
721 Charles C Thomas. P 156-162

722

723 **Lacruz RS, Dean MC, Ramirez-Rozzi F, Bromage TG** (2008) Megadontia, striae periodicity and
724 patterns of enamel secretion in Plio-Pleistocene fossil hominins. *J Anat.* **213**, 148–158

725

726 **Lacruz RS, Bromage TG** (2006) Appositional enamel growth in molars of South African fossil
727 hominids. *J Anat* **209**, 13–20.

728

729 **Lacruz RS, Hacia JG, Bromage TG. et al.** (2012) The circadian clock modulates enamel
730 development. *J Biol Rhyth* **27**, 237–245.

731

732 **Lee CF, Profitt WR** (1995) The daily rhythm of tooth eruption. *Am J Orthod Dentofacial Orthop*
733 **107**(1), 38-47.

734

735 **Li C, Risnes S** (2004) SEM observations of Retzius lines and prism cross-striations in human dental
736 enamel after different acid etching regimes. *Arch Oral Biol* **49**, 45-52.

737

738 **Little MA, Rummel JA** (1971) Circadian variations in thermal and metabolic responses to heat
739 exposure. *J Appl Physiol* **31**(4), 556–561.

740

- 741 **Lovejoy CO, Meindl RS, Pryzbeck TR, Mensforth TJ** (1985) Chronological metamorphosis of the
742 auricular surface of the ilium: A new method for the determination of age at death. *Am J Phys*
743 *Anthropol* **68**, 15-28.
- 744
- 745 **Macho G** (1995) The significance of hominid enamel thickness for phylogenetic and life-history
746 reconstruction. In: *Aspects of Dental Biology: Palaeontology, Anthropology and Evolution* (ed.
747 Moggi-Cecchi J), pp. 51–68. Florence: International Institute for the Study of Man.
- 748
- 749 **Mahoney P** (2008) Intraspecific variation in M1 enamel development 601 in modern humans:
750 implications for human evolution. *J Hum Evo* **55**, 131–147.
- 751
- 752 **Mahoney P** (2011) Human deciduous mandibular molar incremental enamel development. *Am J Phys*
753 *Anthropol*, 144, 204–214.
- 754
- 755 **Mahoney P** (2013) Testing functional and morphological interpretations of enamel thickness along
756 the deciduous tooth row in human children. *Am J Phys Anthropol* 151, 518–525.
- 757
- 758 **Mahoney P** (2015) Dental fast track: prenatal enamel growth, incisor eruption, and weaning in human
759 infants. *Am J Phys Anthropol* 156, 407–421.
- 760
- 761 **Mahoney P, Miszkiewicz JJ, Pitfield R, Schlecht SH, Deter C, Guatelli-Steinberg D** (2016)
762 Biorhythms, deciduous enamel thickness, and primary bone growth in modern human children: a test
763 of the Havers-Halberg Oscillation hypothesis. *J Anat* **228**, 919–928.
- 764
- 765 **Mahoney P, Miszkiewicz JJ, Pitfield R, Deter C, Guatelli-Steinberg D** (2017) Enamel biorhythms
766 of humans and great apes: the Havers-Halberg Oscillation hypothesis reconsidered. *J Anat* 230, 272-
767 281.
- 768
- 769 **Mahoney P, Smith TM, Schwartz GT, Dean MC, Kelley J** (2007) Molar crown formation in the
770 Late Miocene Asian hominoids, *Sivapithecus parvada* and *Sivapithecus indicus*. *J Human Evol* **53**,
771 61-68
- 772
- 773 **Martin LB** (1983) Relationships of the later Miocene Hominoidea. Ph.D. Dissertation, University
774 College London.
- 775
- 776 **Martin LB** (1985) Significance of enamel thickness in hominoid evolution. *Nature* **314**, 260-263.
- 777
- 778 **Meindl RS, Lovejoy CO, Mensforth RP, Walker RA** (1985) A revised method of age

779 determination using the os pubis, with a review and tests of accuracy of other current methods of
780 pubic symphyseal aging. *Am J Phys Anth* **68**, 29–45.

781

782 **Metz LN, Martin RB, Turner AS** (2003) Histomorphometric analysis of the effects of osteocyte
783 density on osteonal morphology and remodeling. *Bone* **33**(5), 753-759.

784

785 **Miszkievicz JJ** (2014) Ancient human bone histology and behaviour. PhD Dissertation. University
786 of Kent: Canterbury, UK.

787

788 **Miszkievicz JJ** (2016) Investigating histomorphometric relationships at the human femoral midshaft
789 in a biomechanical context. *J Bone Min Metab* **34**(2), 179-192.

790

791 **Miszkievicz JJ, Mahoney P** (2016) Ancient human bone microstructure in medieval England:
792 comparisons between two socio-economic groups. *Anat Rec* **299**, 42-59.

793

794 **Mullender MG, Huiskes R, Versleyen H, Buma P** (1996) Osteocyte Density and
795 Histomorphometric Parameters in Cancellous Bone of the Proximal Femur in Five Mammalian
796 Species. *J Orth Res* **14**, 972-979.

797 **Mullender MG, Tan SD, Vico L, Alexandre C, Klein-Nulend J** (2005). Differences in osteocyte
798 density and bone histomorphometry between men and women and between healthy and osteoporotic
799 subjects. *Calcif Tiss Int* **77**(5), 291-296.

800 **Nakashima T, Hayashi M, Fukunaga T, Kurata K, Oh-Hora M, Feng JQ, Bonewald LF,**
801 **Kodama T, Wutz A, Wagner EF, Penninger JM, Takayanagi H** (2011) Evidence for osteocyte
802 regulation of bone homeostasis through RANKL expression. *Nat Med* **17**,1231-4.

803 **Newman H, Poole D** (1974) Observations with scanning and transmission electron microscopy on the
804 structure of human surface enamel. *Arch Oral Biol* **19**, 1135-1143.

805

806 **Newman H, Poole D** (1993) *Dental enamel growth*. *J Roy Soc Med* **86**, 61.

807

808 **Noble BS** (2008) The osteocyte lineage. *Arch Biochem Biophys* **473**, 106–111.

809

810 **Ohtsuka-Isoya M, Hayashi H, Shinoda H** (2001) Effect of suprachiasmatic nucleus lesion on
811 circadian dentin increments in rats. *Am J Physiol Reg Integrative Comp Physiol* **280**, 1364-1370.

812

813 **Palumbo C, Palazzini S, Marotti G** (1990) Morphological study of inter-cellular junctions during
814 osteocyte differentiation. *Bone* **11**, 401–406.

815

816 **Parfitt AM** (1983) Steriologic basis of bone histomorphometry; theory of quantitative microscopy
817 and reconstruction of the third dimension. In: *Bone Histomorphometry: Techniques and Interpretation*
818 (Recker RR, ed). pp, 53–87. Boca Raton, FL: CRC Press.

819

820 **Phenice TW** (1969) A newly developed visual method for sexing the os pubis. *Am J Phys Anthropol*
821 **30**, 297-302.

822

823 **Ralph MR, Foster RG, Davis FC, Menaker M** (1990) Transplanted suprachiasmatic nucleus
824 determines circadian period. *Science* **247**, 975–978.

825

826 **Reid DJ, Beynon AD, Ramirez Rozzi FV** (1998) Histological reconstruction of dental development
827 in four individuals from a medieval site in Picardie, France. *J Hum Evol* **35**, 463–477.

828

829 **Reid DJ, Dean MC** (2006) Variation in modern human enamel formation times. *J Hum Evol* **50**,
830 329–346.

831

832 **Reid DJ, Ferrell R** (2006) The relationship between number of striae of Retzius and their periodicity
833 in imbricational enamel formation. *J Hum Evol* **50**, 195–202.

834

835 **Reinberg A, Sidi E, Ghata J** (1965) Circadian reactivity rhythms of human skin to histamine or
836 allergen and the adrenal cycle. *J Allergy* **36**, 273-283.

837

838 **Retzius A** (1837) Bemerkungen über den inneren Bau der Zähne, mit besonderer Rücksicht auf dem
839 in Zahnknochen Vorkommenden Röhrenbau. *Arch Anat Physiol* 486–566.

840 **Richter CP** (1965) *Biological Clocks in Medicine and Psychiatry*. Springfield, IL: CC Thomas.

841

842 **Risnes S** (1986) Enamel apposition rate and the prism periodicity in human teeth. *Scand J Dent Res*
843 **94**, 394–404.

844

845 **Risnes S** (1990) Structural characteristics of staircase-type retzius lines in human dental enamel
846 analyzed by scanning electron microscopy. *Anatom Rec* **226**, 135–146.

847

848 **Risnes S** (1998) Growth tracks in dental enamel. *J Hum Evol* **35**, 331-350.

849

850 **Robling AG, Duijvelaar KM, Geevers JV, Ohashi N, Turner CH** (2001) Modulation of
851 appositional and longitudinal bone growth in the rat ulna by applied static and dynamic force. *Bone*,
852 **29**, 105–113.

853 **Robling AG, Castillo AB, Turner CH** (2006) Biomechanical and molecular regulation of bone
854 remodeling. *Annu Rev Biomed Eng* **8**, 455-498.

855

856 **Robling AG, Turner CH** (2002). Mechanotransduction in bone: genetic effects on
857 mechanosensitivity in mice. *Bone* **31**(5), 562-569.

858

859 **Roche AF** (1992) Growth, maturation and body composition. The Fels longitudinal study 1929-1991.
860 Cambridge University Press.

861

862 **Schour I, Poncher HG** (1937) Rate of apposition of enamel and dentin, measured by the effect of
863 acute fluorosis. *Am J Dis Child* **54**, 757-776.

864

865 **Schwartz GT, Mahoney P, Godfrey LR, Cuzzo FP, Jungers WL, Randria GFN** (2005) Dental
866 development in *Megaladapis edwardsi* (primates, lemuriformes): implications for understanding life
867 history variation in subfossil lemurs. *J Hum Evol* **49**, 702-721.

868

869 **Schwartz GT, Reid DJ, Dean C** (2001) Developmental aspects of sexual dimorphism in hominoid
870 canines. *Int J Primatol* **22**, 837-860.

871

872 **Schwartz GT, Samonds KE, Godfrey LR, Jungers WL, Simons EL** (2002) Dental microstructure
873 and life history in subfossil Malagasy lemurs. *Proc Natl Acad Sci USA* **99**, 6124-6129.

874

875 **Schwartz JH** (1995) *Skeleton Keys*. Oxford University Press.

876

877 **Smith TM** (2008) Incremental dental development: methods and applications in hominoid
878 evolutionary studies. *J Hum Evol*, **54**, 205-224.

879

880 **Smith TM, Dean MC, Kelley J, Martin LB, Reid DJ, Schwartz GT** (2003) Molar crown formation
881 in Miocene hominoids: a preliminary synthesis. *Am J Phys Anthropol.* **36** (Suppl.), 196.

882

883 **Somner W** (1703) *The antiquities of Canterbury*. EP Publishing Limited.

884

885 **Sothorn RB** (1974) Chronobiologic serial section on 8876 oral temperatures collected during 4.5
886 years by presumably healthy man (age 20.5 at start of study). In *Chronobiology* (eds Scheving LE,
887 Halberg F, Pauly JE), pp. 245-248. Tokyo: Igaku Shoin Ltd.

888

889 **Sujino M, Masumoto K, Yamaguchi S, van der Horst GT, Okamura H, Inouye SI** (2003)
890 Suprachiasmatic nucleus grafts restore circadian behavioral rhythms of genetically arrhythmic mice.
891 *Curr Biol* **13**(8), 664–668.
892

893 **Tanner JM** (1990) *Fetus into man: physical growth from conception to maturity*. Cambridge, MA:
894 Harvard University Press.
895

896 **Tatsumi S, Ishii K, Amizuka N, Li M, Kobayashi T, Kohno K, Ito M, Takeshita S, Ikeda K**
897 (2007) Targeted ablation of osteocytes induces osteoporosis with defective mechanotransduction. *Cell*
898 *Metab* **5**, 464–75.
899

900 **Teti A, Zallone A** (2009) Do osteocytes contribute to bone mineral homeostasis? Osteocytic
901 osteolysis revisited. *Bone* **44**, 11–16.
902

903 **Trotter M** (1970) Estimation of stature from intact long bones. In *Personal Identification in Mass*
904 *Disasters* (eds Stewart TD), pp. 71–83. Washington, DC: Smithsonian Institution Press.
905

906 **Verborgt O, Gibson GJ, Schaffler MB** (2000) Loss of osteocyte integrity in association with
907 microdamage and bone remodeling after fatigue in vivo. *J Bone Miner Res* **15**, 60–7.
908

909 **van Hove RP, Nolte PA, Vatsa A, Semeins CM, Salmon PL, Smit TH, Klein-Nulend J** (2009)
910 Osteocyte morphology in human tibiae of different bone pathologies with different bone mineral
911 density—is there a role for mechanosensing? *Bone* **45**(2), 321–329.
912

913 **Weaver D** (1998) The Suprachiasmatic Nucleus: A 25-Year Retrospective. *J Biol Rhythms* **13**(2):
914 100–112.
915

916 **White T D, Black MT, Folkens PA** (2011) *Human Osteology*. 3rd ed. Boston: Academic Press.
917

918 **Wolff J** (1982) *Das Gesetz der Transformation der Knochen*. Berlin: Hirschwald.
919

920 **Zheng L, Seon YJ, Mourão MA. et al.** (2013). Circadian rhythms regulate amelogenesis. *Bone* **55**,
921 158–165.
922
923
924
925
926

927
928
929
930
931
932
933
934
935
936
937
938
939
940
941
942
943
944
945
946
947
948
949
950
951
952
953
954

Author Manuscript

Table 1 Linear regression analyses of log-Retzius periodicity against log-enamel growth.

ENAMEL	<i>n</i>	Intercept	Slope	<i>r</i>	<i>r</i>²	<i>p</i>	Residual
<i>Thickness. RP v EA</i>							
All	40	0.755	0.569	0.697	0.486	<0.001*	55%
M1	25	0.826	0.489	0.615	0.378	0.001*	64%
M2	15	0.639	0.703	0.806	0.650	<0.001*	43%

Thickness. RP v AET

All	40	-0.426	0.432	0.604	0.365	0.002*	63%
M1	25	-0.391	0.384	0.577	0.333	0.004*	68%
M2	15	-0.542	0.580	0.720	0.519	0.002*	44%

Rate. RP v DSR

M1	15	0.817	-0.098	0.009	0.000	0.714	98%
----	----	-------	--------	-------	-------	-------	-----

955 Tooth types: M1, permanent first molar; M2, permanent second molar. *Significant. EA:
956 Enamel area. AET: Average enamel thickness. DSR: Daily secretion rate. RP: Retzius
957 periodicity. **RP v EA**: Lower M1 ($n=13$): $r^2=0.491$, $p=0.007^*$. Upper M1 ($n=12$): $r^2=0.633$,
958 $p=0.001^*$. Lower M2 ($n=12$): $r^2=0.603$, $p=0.002^*$. **RP v AET**: Lower M1 ($n=13$): $r^2=$
959 0.338 , $p=0.037^*$. Upper M1 ($n=12$): $r^2=0.482$, $p=0.012^*$. Lower M2 ($n=12$): $r^2=0.287$, $p=$
960 0.072 . Upper M2 excluded from separate analysis as $n=3$.

961
962
963
964
965
966
967
968
969
970
971
972
973
974
975

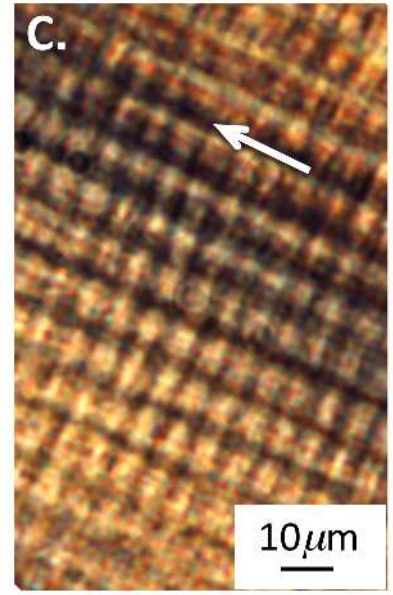
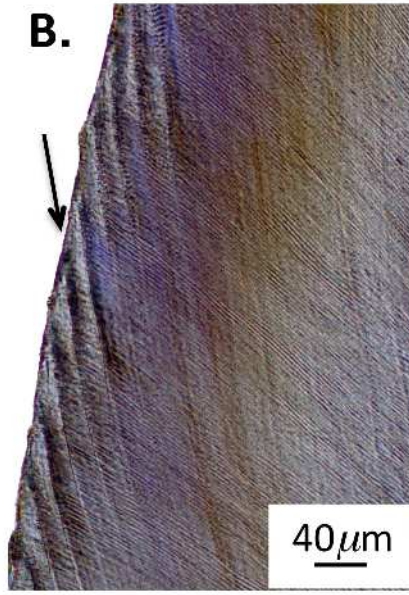
BONE	<i>n</i>	Intercept	Slope	<i>r</i>	<i>r</i>²	<i>p</i>	Residual
<i>Stature. RP v S^a</i>							
Younger M	27	2.309	-0.082	-0.417	0.213	0.015*	74%
<i>Rate. RP v Ot.Dn</i>							
Younger M	10	3.232	-0.401	-0.370	0.159	0.326	90%
<i>Rate. S v Ot.Dn^b</i>							
Younger M	28	2.171	0.019	0.199	0.039	0.317	94%
Older M	94	2.185	0.016	0.175	0.030	0.089	93%

Table 2 Linear regression analyses of log-Retzius periodicity against log-bone growth.

977 S: Estimated stature. RP: Retzius periodicity. M: Males. Ot.Dn: Osteocyte lacunae density.

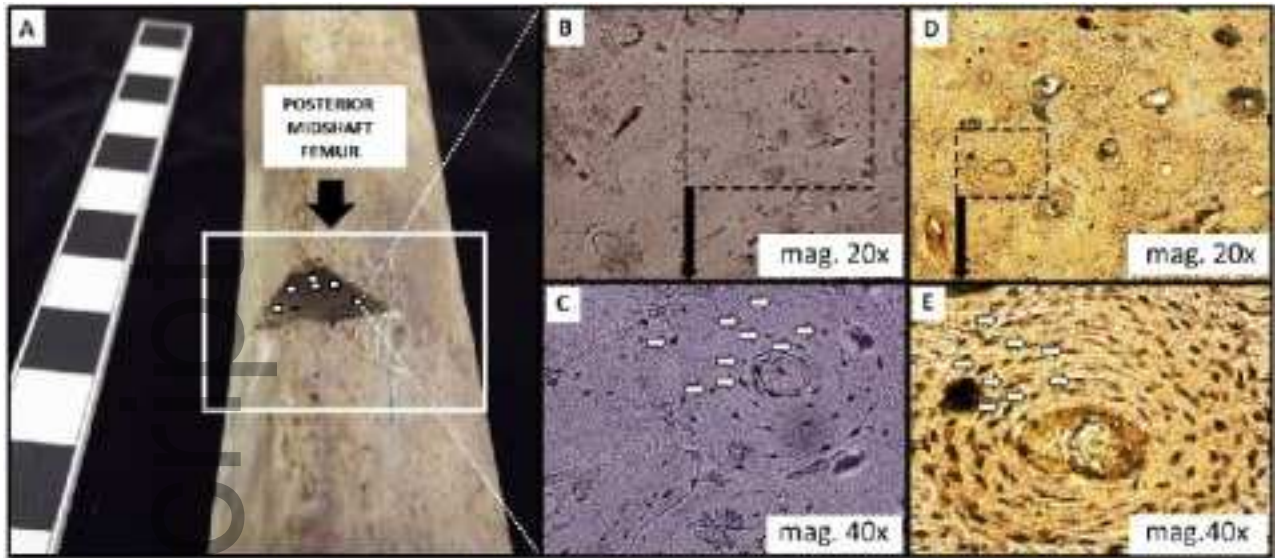
978 ^aFemoral length v RP: Young M intercept= 3.232, slope= -0.135, r=-0.492, *p*=0.020*.

979 ^bOt.Dn v femoral length: Young M intercept= 1.567, slope= 0.030, r=0.199, *p*=0.317. Older
980 M intercept= 1.587, slope= 0.025, r=0.176, *p*=0.088.



joa_12709_f1.tif

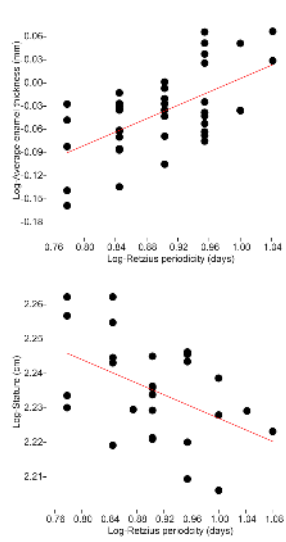
Author Manuscript



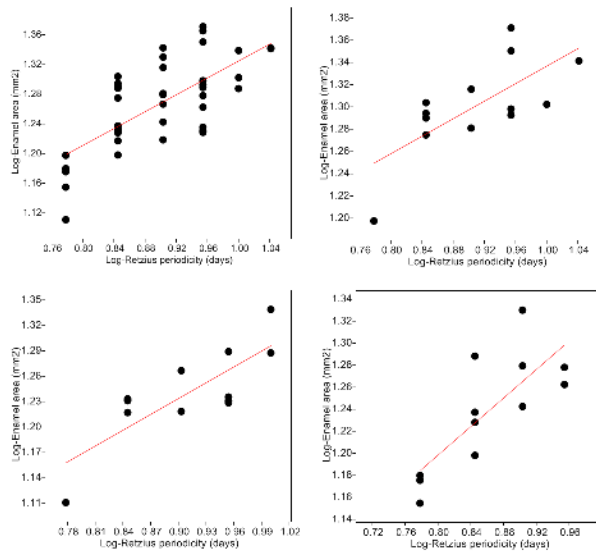
joa_12709_f2.tif

Author Manuscript

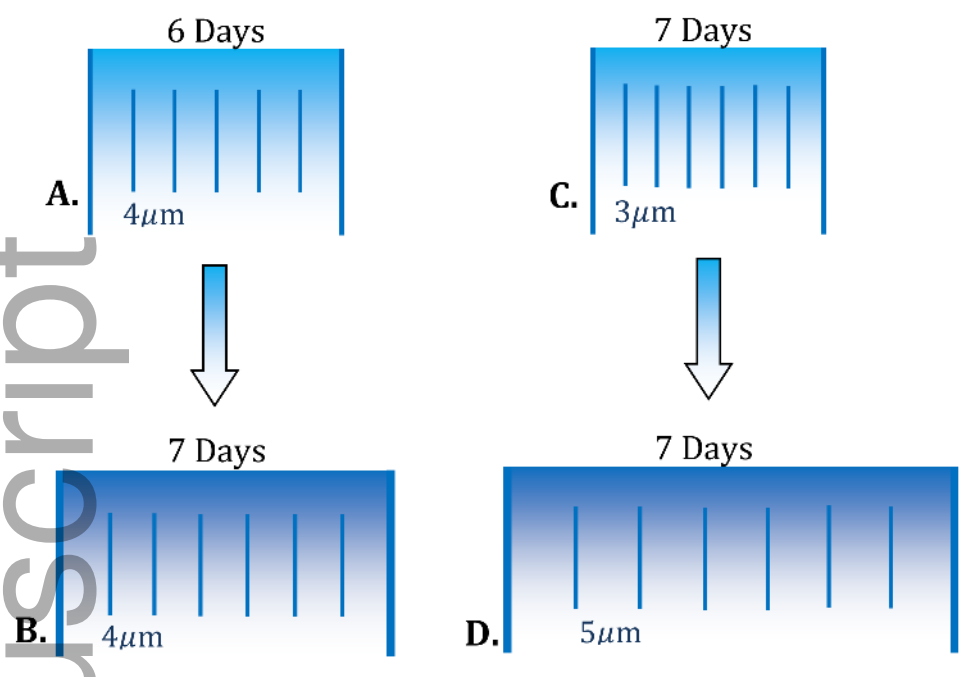
Author Manuscript



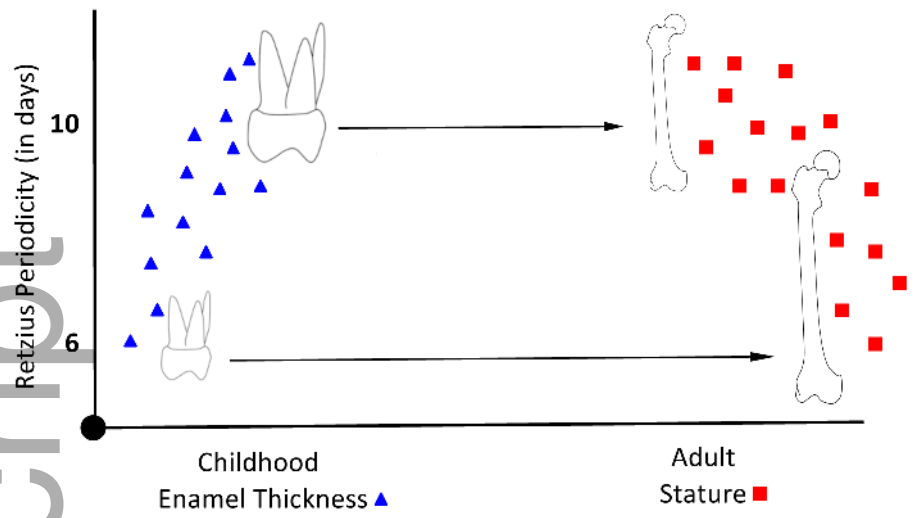
joa_12709_f3.tif



joa_12709_f4.tif



joa_12709_f5.tif



joa_12709_f6.tif